COUPLED CASMO5-VIPRE ANALYSIS OF NON-UNIFORM VOID DISTRIBUTIONS IN BWR LATTICES

Joshua Hykes, Gerardo Grandi, Rodolfo Ferrer, and Joel Rhodes*
Studsvik Scandpower, Inc.
1070 Riverwalk Drive, Suite 150
Idaho Falls ID 83402, USA
joshua.hykes@studsvik.com, gerardo.grandi@studsvik.com,
rodolfo.ferrer@studsvik.com, joel.rhodes@studsvik.com

ABSTRACT

This paper describes the CASMO5 portion of an ongoing effort at Studsvik to quantify the effects of radially non-uniform void distributions (NVD) in BWR fuel bundles using the CASMO5-SIMULATE5 nuclear fuel analysis tools. The two questions addressed here are: (1) How much axial detail is needed in the thermal-hydraulics subchannel model to achieve an accurate void fraction distribution? and (2) How much do the eigenvalue and pin powers computed by CASMO5 change when accounting for the NVD as compared to the uniform void distribution (UVD)? The NVD is computed using the subchannel analysis code VIPRE. The void and pin powers are coupled with a fixed-point iteration scheme between CASMO5 and VIPRE. To answer question (1), a set of VIPRE results is presented varying the axial power shape and the height of the slice of interest. The axial power shape has a negligible effect on the NVD, while the axial height does have a small influence on the NVD. To answer question (2), a set of numerical results is presented for an 8-by-8 BWR lattice with two small water rods. For lattices with 12 gadolinium poisoned pins at 8 weight percent, the δk with respect to the uniform void reference has a peak near the burnout of gadolinium, with a peak-to-peak amplitude of 400–600 pcm for the 20 and 40% average void cases. The δk is smaller for 80% average void and the gadolinium-free lattices. Near zero burnup when the peaking factors are the highest, accounting for the NVD tends to flatten the pin power distribution, reducing the power by up to 2% in some of the high-power pins.

Key Words: **void, BWR, CASMO, VIPRE**

1. INTRODUCTION

Gadolinium-poisoned fuel pins, water rods, and the channel box wall create colder surfaces in BWR bundles as compared to a typical fuel pin. These cold surfaces reduce the boiling in the adjoining subchannels, thereby creating a non-uniform void distribution (NVD), with greater void near the hot fuel pins.

*studsvik.com/nfa

Ikehara et al. summarizes a number of previous studies of this effect [1], as well as performing a three-dimensional analysis of a BWR bundle using TGBLA or MCNP4C for neutronics and COBRAG for the thermal-hydraulics (T/H) calculation. The authors report a maximum change in eigenvalue of $\pm 0.6\% \delta k$ for a lattice at 40% average void during a depletion calculation.

Studsvik is interested in quantifying the effect of the bundle NVD for reactor core analysis using CMS5, Studsvik's current nuclear fuel analysis code package. The two primary components of CMS5 are the 2D lattice-physics code CASMO5 [2] and the nodal core simulator SIMULATE5 [3]. In the process of quantifying the NVD effect at the core level, the following questions must be addressed:

1. What level of axial detail is necessary in the 3D T/H subchannel simulation? To answer the following questions, the NVD must be treated by CASMO5, which is a 2D simulation. If there is a strong dependence on the axial detail of the subchannel model, then additional work may be required in CASMO5 to capture the axial dependence.
2. Is the effect of NVD noticeable in the CASMO5 depletion results? If the NVD model does not change the lattice physics results, then it should not be important at the core level either.

Question 1 is answered in section 2. The 3D axial details are found to have negligible to small effects on the NVD. Sample results to answer question 2 are given in section 3.

2. IMPORTANCE OF AXIAL DETAILS IN SUBCHANNEL T/H MODEL FOR NVD

While the lattice physics calculation of CASMO5 is in the radial plane of a fuel bundle, the T/H subchannel analysis requires an axial description of the bundle. To avoid introducing axial dependencies in the lattice physics calculation, we test if a simplified axial description for the subchannel model is sufficient to generate an accurate NVD. The main simplifications we consider are for the radial pin powers, the axial power shape, and the axial height below the plane of interest.

2.1. Radial Pin Powers

In BWR fuel bundles, the enrichment and poison pin layouts change as a function of the axial height. This implies that the radial pin power shape will change as a function of height. However, for the present study, we assume that the radial pin power distribution is the same throughout the assembly. This assumption is consistent with the 2-step lattice physics/nodal simulator approach to core analysis. Relaxing this assumption would greatly increase the complexity of an NVD model in CMS5.

The simulation [1] from Ikehara et al. of a 3D fuel bundle included axially-varying radial pin powers, which could serve as reference for the present 2D models.

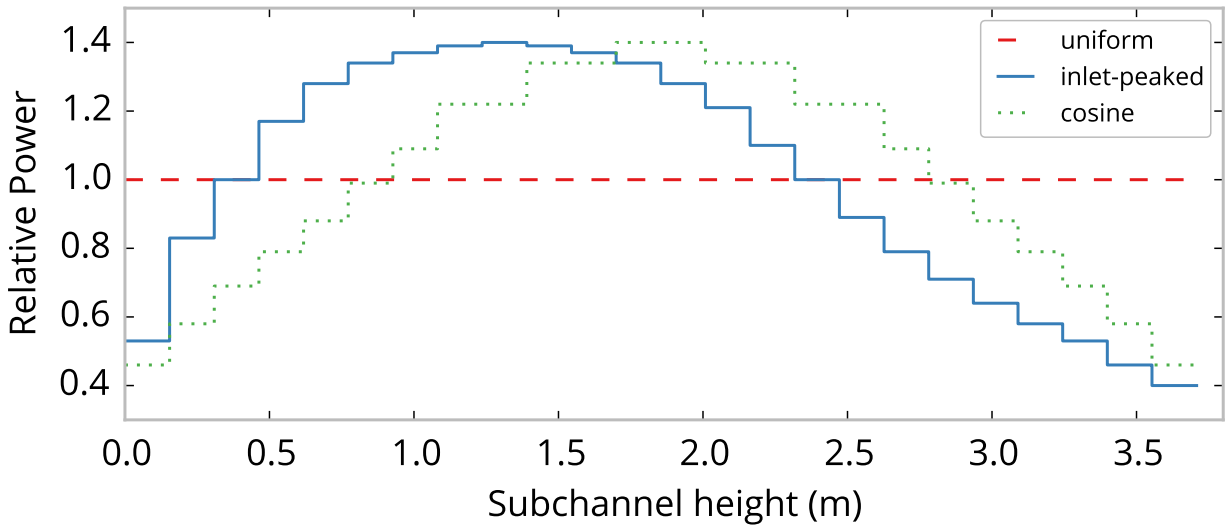

Figure 1: The three axial power shapes considered.

2.2. Axial Power Shape

The subchannel model must include an axial power shape. Three candidate axial shapes are considered:

- Uniform – simplest
- Cosine – simple but closer to the power shape in a theoretical cylindrical reactor
- Inlet-peaked – typical of a BWR axial power shape

The axial power shapes considered are shown in Figure 1. To quantify this effect, the three power shapes were provided as input to VIPRE [4], the subchannel analysis code, with otherwise identical input. The radial pin power distribution was copied from a zero-burnup CASMO5 calculation similar to the configuration described in subsection 3.2. The total subchannel height was about 3.7 m, split into 24 axial nodes. The total assembly power was adjusted to produce an exiting average void fraction of 40%.

Comparisons of the NVD at the channel exit for the three power shapes are given in Figure 2. The change in NVD between the three shapes is negligible (less than 0.01 change for voids ranging from 0.25 to 0.5), so we use the simplest uniform power shape in all of the following subchannel analysis.

2.3. Axial Height

Figure 3 compares the NVDs for full (3.7 m) and half (1.9 m) bundle heights. The subchannel model is similar to the previous section, but uses the uniform axial power shape. The effect of the axial height is

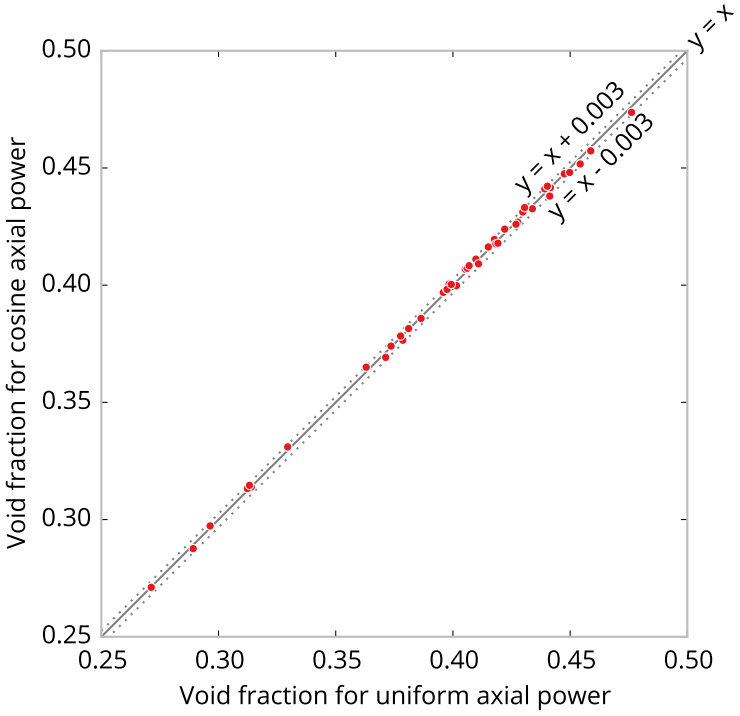

(a) Cosine versus uniform

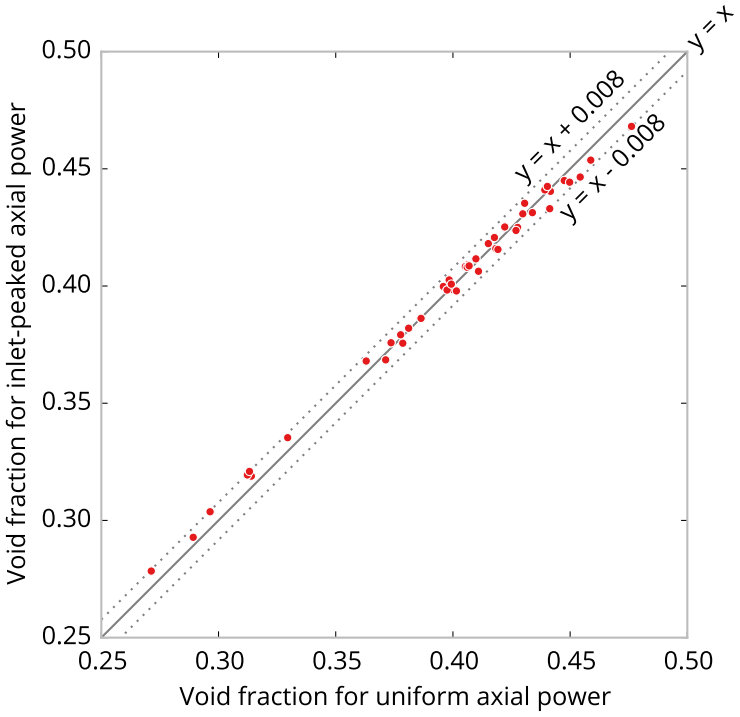

(b) Inlet-peaked versus uniform

Figure 2: Comparison of the NVDs for the uniform, cosine, and inlet-peaked axial power shape.

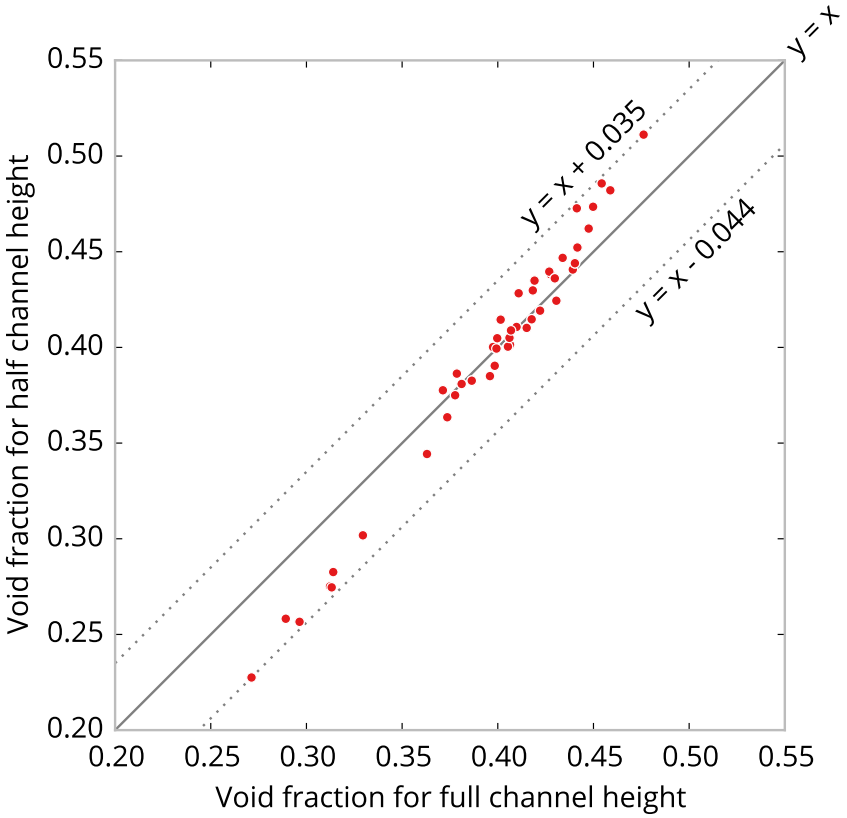

Figure 3: Comparison of the NVDs for the full and half-height subchannels.

small (a maximum of about 0.05 change for a range of voids of 0.25 to 0.5). The half-height case has a more peaked void distribution than the full-height case. The range of voids is about 0.23–0.52 for the half-height case, and 0.27–0.47 for the full-height case. This makes physical sense – the longer flow path allows for more mixing and a flatter NVD.

Considering the important lattices near the middle of the bundle, the approximation of using the full bundle height in the subchannel analysis yields a flatter NVD estimate than what the true height would produce. The magnitude of the change (< 0.05) is relatively small compared to the range of voids present (0.25–0.5); therefore, we will accept this approximation for now. However, it may merit further consideration at later stages in the development of the NVD model.

3. NVD EFFECT ON 2D LATTICE DEPLETION

Having seen in section 2 that a simplified axial description for the subchannel model is tenable, we turn now to quantify the effect of the NVD on the depletion of a sample BWR lattice.

3.1. Methods

CASMO5 computes the radial pin power distribution for a given NVD (or simply a uniform void, which is the default). The subchannel analysis code VIPRE computes the NVD for a given radial pin power distribution. The codes are coupled with fixed point iteration as described in Algorithm 1.

Algorithm 1 Void-power coupling iteration

1: **for** statepoint in depletion **do**
2: Guess initial void distribution (flat or from previous statepoint).
3: **while** $\epsilon > \tau_r$ **do**
4: Compute pin powers in CASMO5 with current void distribution.
5: Compute void distribtion in VIPRE with updated pin powers.
6: Compute pin power convergence parameter $\epsilon = \max_i \frac{|p_i^{\text{old}} - p_i^{\text{new}}|}{p_i^{\text{new}}}$.
7: **end while**
8: Deplete to next statepoint.
9: **end for**

Two values for the stopping criterion were tested. A loose stopping criterion was set as $\tau_r = 0.003$. At most statepoints, only two iterations were needed to fulfill the loose stopping criterion. A tighter criterion was set as $\tau_r = 10^{-4}$, but the results were in general only minimally different than those with the looser stopping criterion. A few pincell voids were noticeably different, so the results using the tighter stopping criterion are presented here.

VIPRE gives the void distribution in terms of the subchannels, with a typical interior subchannel in contact with four fuel pins. However, CASMO5 uses a pincell discription of the void distribution. Therefore, after parsing the void distribution from the VIPRE output file, it is converted from per-subchannel to per-pincell using an area-weighted sum,

$$\alpha_p = \frac{\sum_{s \in p} \alpha_s A_s f_{s \in p}}{\sum_{s \in p} A_s f_{s \in p}} \tag{1}$$

where

$$\alpha_p = \text{void fraction in pincell } p \tag{2}$$
$$\alpha_s = \text{void fraction in subchannel } s \tag{3}$$
$$A_s = \text{area of subchannel } s \tag{4}$$
$$f_{s \in p} = \text{fraction of subchannel } s \text{ area in pincell } p \tag{5}$$

The summations are taken over all subchannels s which overlap with pincell p. The $f_{s \in p}$ factor is $1/4$ for interior subchannels, $1/2$ for boundary subchannels not on the corners, and 1 for the corner subchannels.

3.2. Results

A set of test problems was analyzed based on an 8-by-8 BWR lattice design from the BFBT report [5]. This lattice has two small water rods near the center. Three pin layouts are considered:

1. No gadolinium pins present. The uranium enrichments range from 2–4 weight percent.
2. Similar to 1, but with 12 gadolium-poisoned pins evenly dispersed in the lattice. The locations of these pins are shown in red in Figure 4c. This is called the "dispersed Gd" pattern. The gadolinia content in the Gd pins is 8 weight percent.
3. Similar to 2, but the gadolinium pins are concentrated near one corner of the lattice, forming a clump of Gd pins. This is called the "clumped Gd" pattern.

The pin maps are pictured in Figure 4. Each layout is analyzed at 20, 40, and 80% void. All lattices are unrodded.

Figure 5 shows the eigenvalues for the NVD cases as compared to the analogous UVD case. With no gadolinium pins (Figure 5a), the δk is negative by approximately 100–200 pcm, diminishing toward higher burnups. While δk is relatively constant for much of the depletion, it has a sharp jump of almost 100 pcm from the first to second statepoint. (The rapid fall in k from the first to second statepoint is caused mostly by the presence of xenon in the second statepoint.)

The shape of δk changes markedly with the introduction of gadolinium pins (Figure 5b and Figure 5c), where the δk is negative for the start and end of the depletion, but turns positive preceding the reactivity peak around 20 MWd/kgU. The peak-to-peak amplitude of δk is 400–600 pcm for the lattices with Gd at 20 and 40% void, with smaller amplitude for 80% void. The shape of δk is similar between the dispersed and clumped Gd patterns. The magnitude and shape of these changes are similar to those reported by Ikehara [1] (in particular, see the $\delta k/k^{\text{hist}}$ curve in Figure 18 therein).

Figure 6 shows the change in pin powers throughout the lattice depletions for NVD versus UVD. Early in the depletion, increases in low power pins of almost 5% and decreases in high power pins of about 2% are observed. (The right figure in Figure 7a shows that the power in the high power pins is being suppressed by NVD while it is increased in the low power pins. At higher burnups where the peaking factors are lower, this is not the case.) Similar to the δk results, the pin power changes for the Gd-free lattice are relatively flat over the depletion. For the lattices with Gd pins, the pin power changes are greatest early in the depletion, decreasing to a minimum around 20 MWd/kgU, and then increasing slightly through the rest of the depletion. The particular layout of the Gd pins (dispersed versus clumped) has only a small effect on pin power changes.

The NVD and pin power maps are shown in Figure 7 for the dispersed Gd layout at 40% void. Early in the depletion, the NVD is depressed in the center of the lattice by the lower pin powers in that area. The hot pins along the boundaries drive relatively high voids along the channel walls. As the bundle burns out, the NVD flattens along with the pin powers.

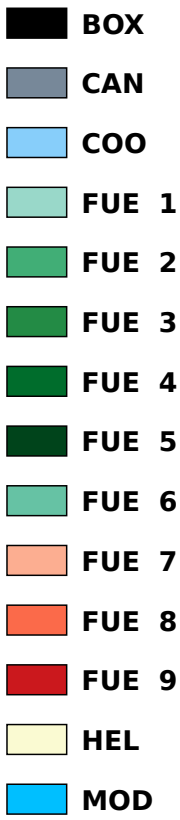

(a) Color key

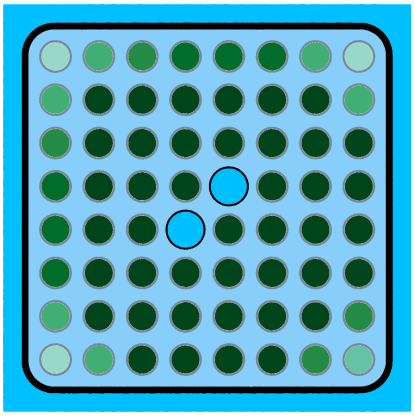

(b) Gd-free pattern

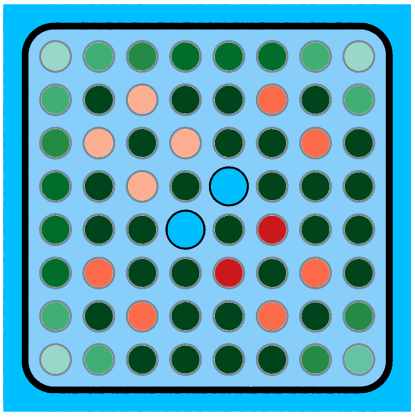

(c) Dispersed Gd pattern

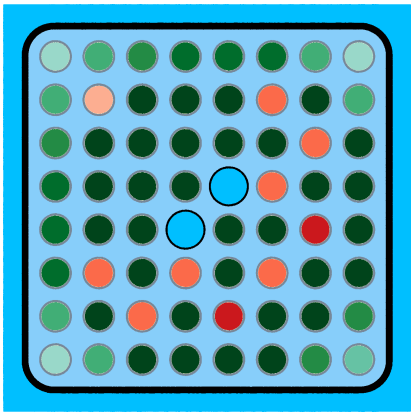

(d) Clumped Gd pattern

Figure 4: Fuel pin layouts for the three example lattices. Gadolinium is present in FUEs 7, 8, and 9. Darker shades represent higher U-235 enrichments.

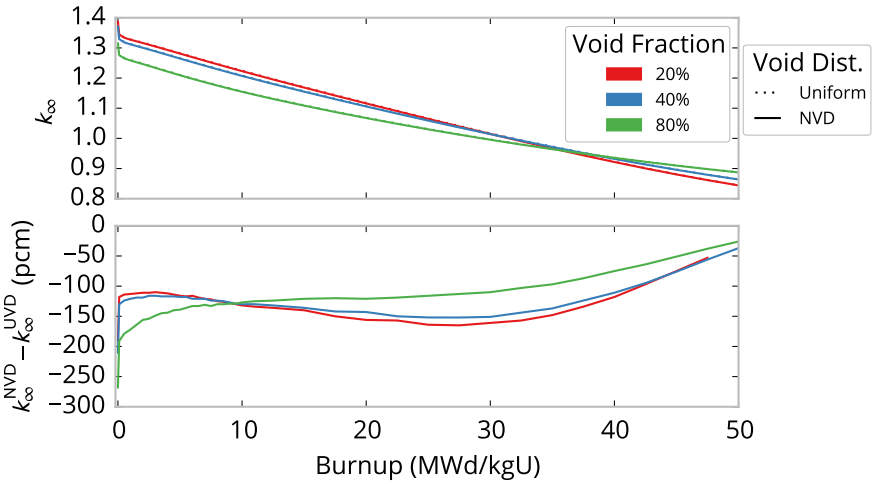

(a) No Gd pattern.

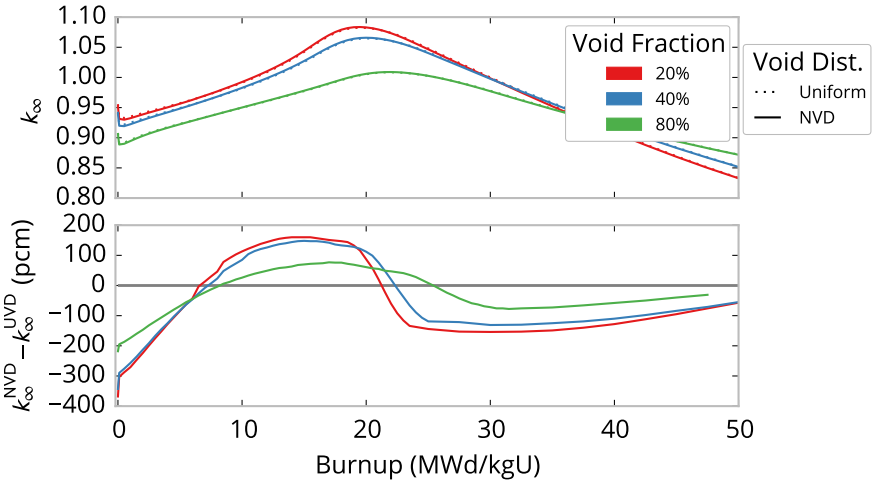

(b) Dispersed Gd pattern.

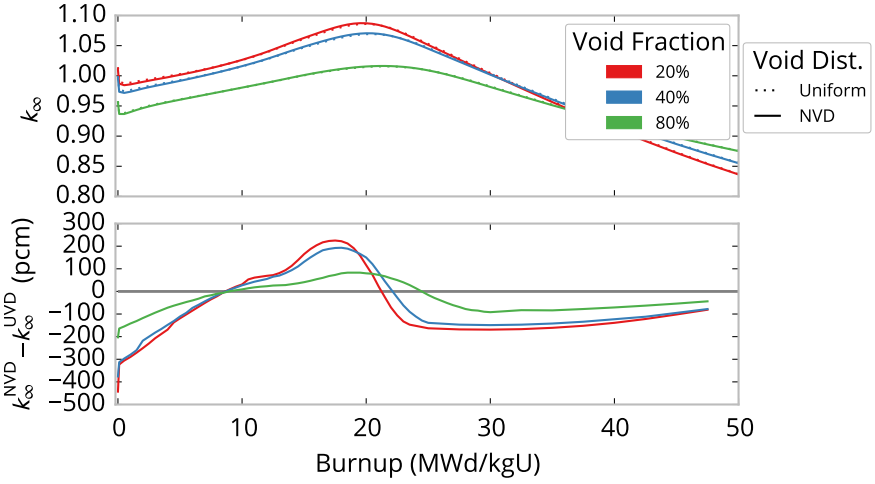

(c) Clumped Gd pattern.

Figure 5: Comparison of the UVD and NVD lattice eigenvalues throughout the depletion of the three lattice configurations at 20, 40, and 80% average void.

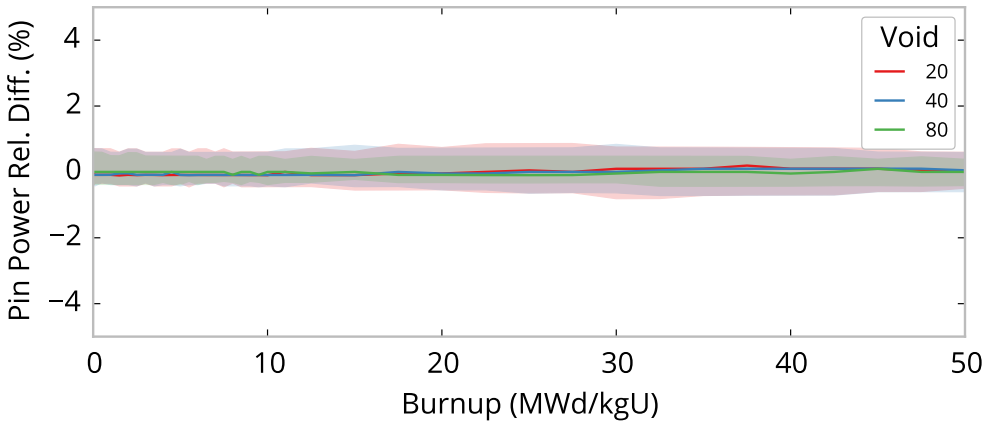

(a) No Gd pattern

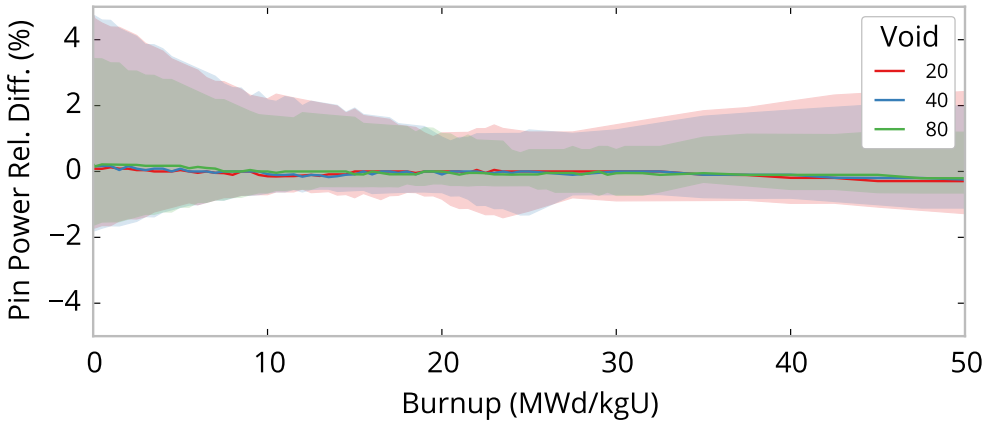

(b) Dispersed Gd pattern

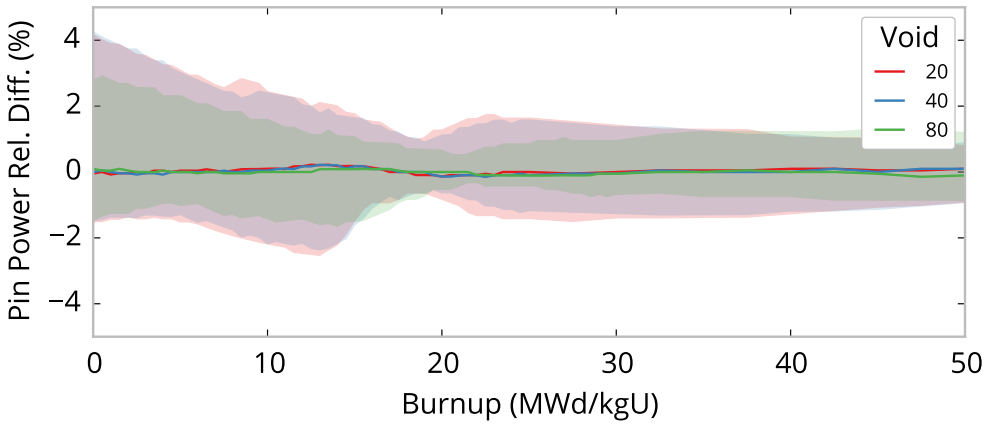

(c) Clumped Gd pattern

Figure 6: Comparison of pin power differences between the NVD and UVD cases. The relative difference is computed as (NVD-UVD)/UVD·100%. The dark central line represents the median relative difference among all the pins, and the transparent shaded region bounds the minimum and maximum relative differences.

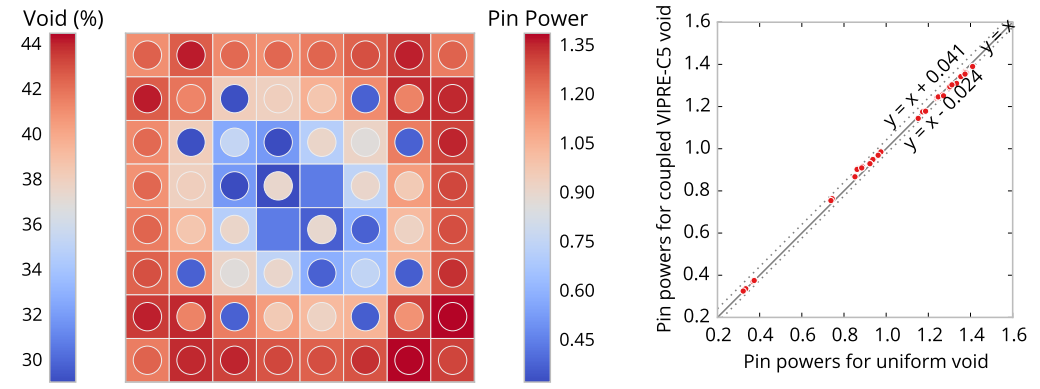

(a) 0 MWd/kgU

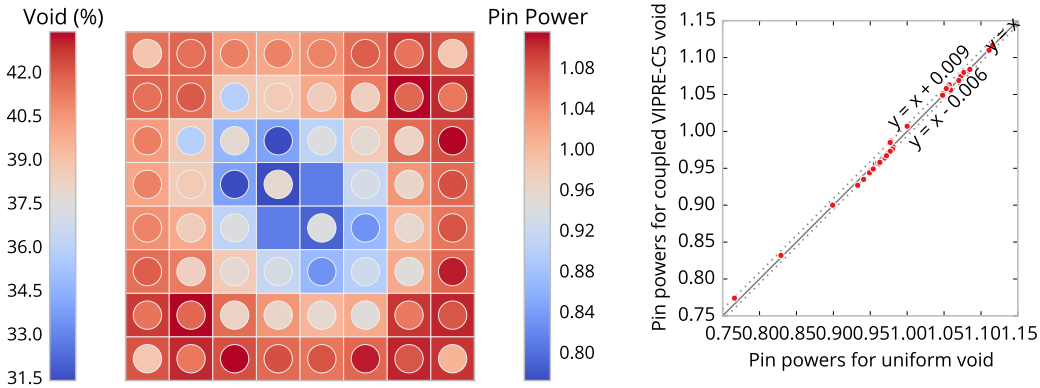

(b) 20 MWd/kgU

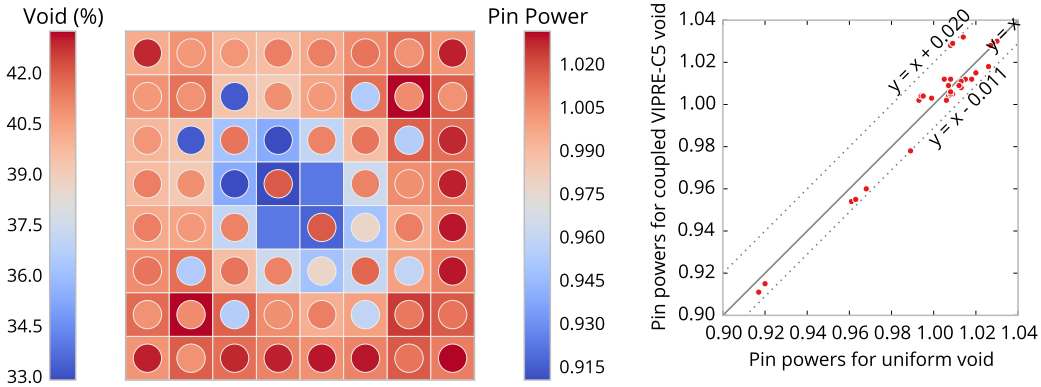

(c) 50 MWd/kgU

Figure 7: Void distribution and pin powers for the dispersed Gd lattice at 40% average void (left column) and UVD versus NVD pin power comparisons (right column). In the left column, the pin powers are represented by the color inside each circle, while the void is represented by the color inside each square pincell but outside the circle.

4. CONCLUSIONS

For gadolinium-free lattices, the effect on k of the NVD is modestly negative throughout the depletion and relatively constant. For lattices with gadolinium pins, the effect on k is negative at the beginning and end of the depletion, but turns positive near the reactivity peak. The effect is most pronounced at 20% and 40% void, although it is still present at 80% void. In several cases, the reactivity swing introduced by NVD is 400–600 pcm.

In terms of pin powers, as expected the NVD does flatten the pin power distribution. Near zero burnup where the pin power peaking is highest, reductions of up to 2% are observed in some of the hottest pins.

Since the changes in k look similar across the different lattice Gd pin layouts, it is possible that these effects might be visible at the nodal core simulator level. Enabling this or a similar void distribution model for the CASMO5 case matrix calculation is ongoing work. This would allow the evaluation of these effects at the core level.

REFERENCES

[1] T. Ikehara *et al.* "Effect of subchannel void fraction distribution on lattice physics parameters for boiling water reactor fuel bundles." *Journal of Nuclear Science and Technology*, **45(12)**: pp. 1237–1251 (2008).

[2] J. Rhodes, K. Smith, and D. Lee. "CASMO5 development and applications." In: *PHYSOR 2006* (2006).

[3] T. Bahadir and S.-Ö. Lindhal. "Studsvik's next generation nodal code SIMULATE-5." In: *ANFM IV* (2009).

[4] C. Stewart *et al. VIPRE-01 – A Thermal-Hydraulic Code for Reactor Cores. Technical Report NP-2511-CCM-A* (2011).

[5] B. Neykov *et al. NUPEC BWR Full-size Fine-mesh Bundle Test (BFBT) Benchmark, Volume I: Specifications. Technical Report NEA/NSC/DOC(2005)5* (2005).